Electronic Supplementary Information (ESI)

Active structure preservation method for developing functional graphitic carbon dots: effective antibacterial agent, sensitive pH and Al(III) nanosensor

Peng Hou,[a] Tong Yang,[a] Hui Liu ,*[a] Yuan Fang Li[b] and Cheng Zhi Huang*[a]

[a] *Key Laboratory of Luminescent and Real-Time Analytical Chemistry (Southwest University), Ministry of Education, College of Pharmaceutical Science, Southwest University, Chongqing 400715, China.*

[b] *College of Chemistry and Chemical Engineering, Southwest University, Chongqing 400715, China.*

*Corresponding author. E-mail: liuhui78@swu.edu.cn, chengzhi@swu.edu.cn;

FAX:+86 23 68367257; Tel: +86 23 68254659;

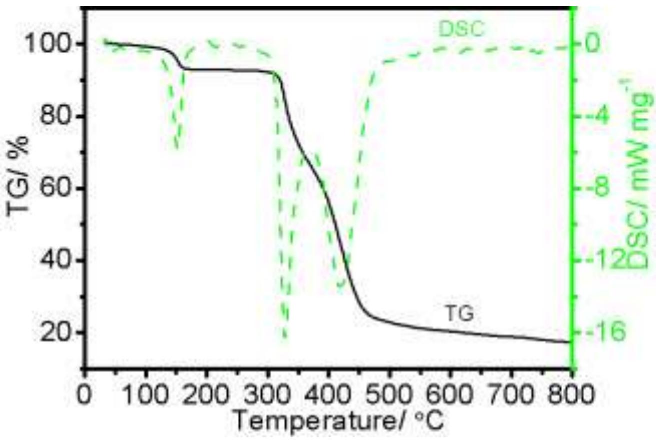

Fig. S1 DSC and TG curve for ciprofloxacin hydrochloride in a dynamic nitrogen atmosphere, respectively, at 30 ml min^{-1} at a heating rate of 10 ºC min^{-1}.

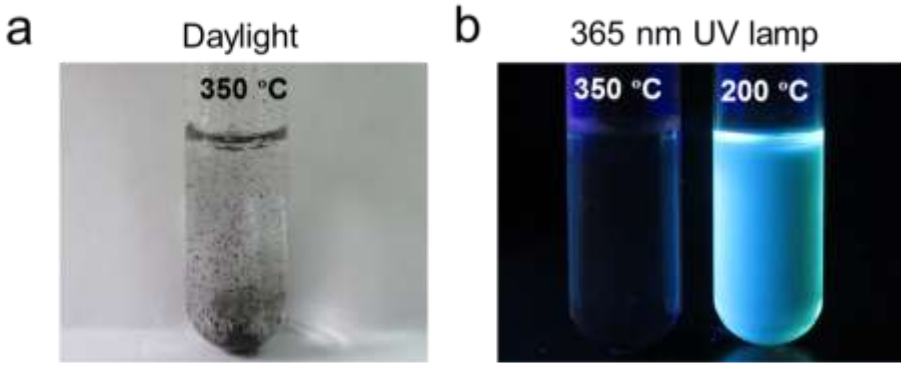

Fig. S2 The obtained product prepared from ciprofloxacin. Photographs of the final product prepared at 350 ºC under daylight (a) and 365 nm UV lamp (b) (using the g-CDs obtained at 200 ºC as reference).

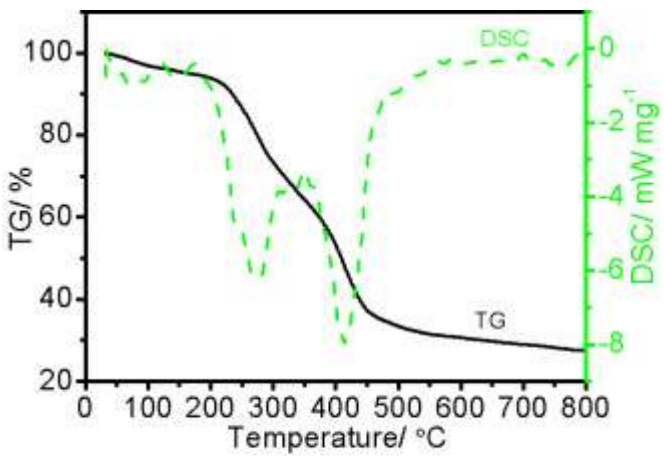

Fig. S3 DSC and TG curve for g-CDs in a dynamic nitrogen atmosphere, respectively, at 30 ml min^{-1} at a heating rate of 10 ºC min^{-1}.

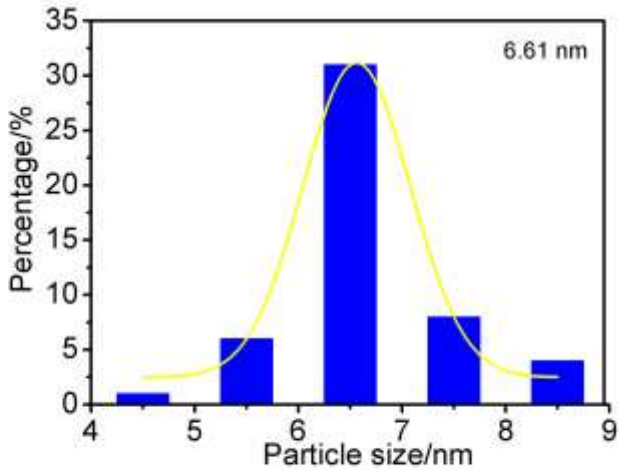

Fig. S4 Size distribution of g-CDs and curve fit to the data using a Gaussian model.

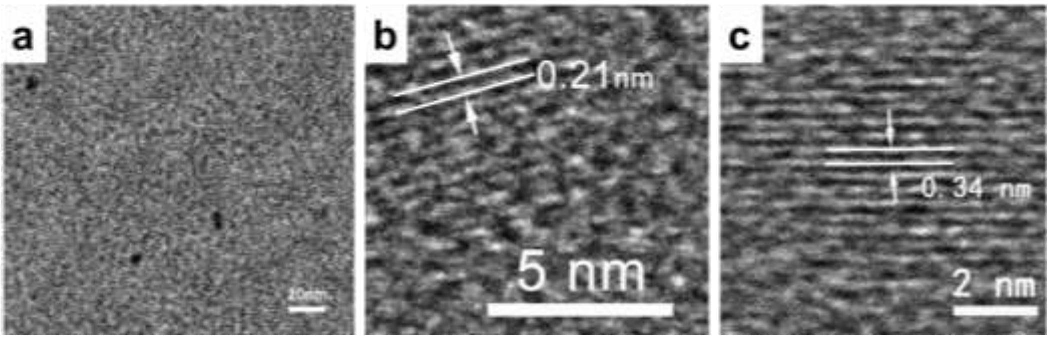

Fig. S5 TEM (a) and HRTEM (b and c) images of g-CDs.

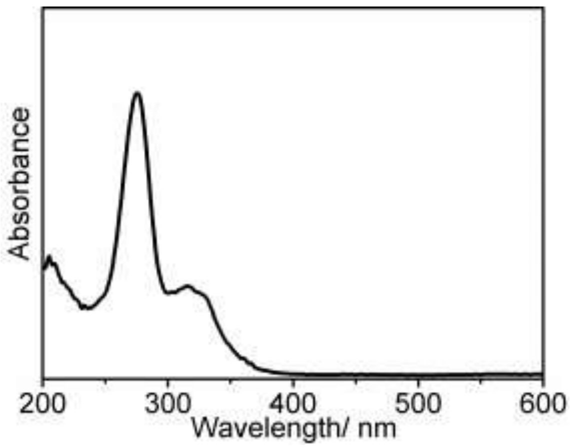

Fig. S6 The UV-vis absorption spectrum of ciprofloxacin hydrochloride.

g-CDs λ_{ex}= 338 nm in water　　　　Quinine sulfate λ_{ex}= 338 nm in 0.1 M H_2SO_4

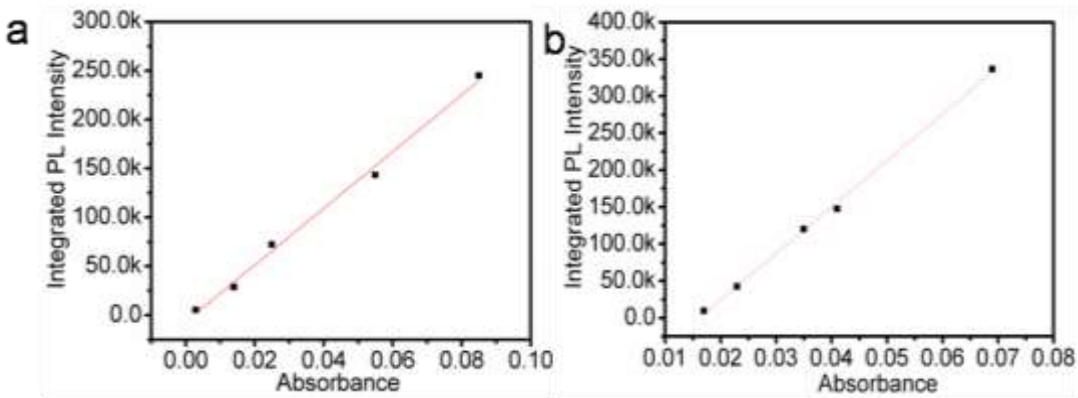

Fig. S7 Plots of integrated fluorescence intensity versus absorbance of the g-CDs and quinine sulfate.

Table S1 The absorption intensity and PL intensity of g-CDs.

g-CDs	1	2	3	4	5
Abs	0.085	0.055	0.025	0.014	0.003
Integrated PL	244724.16	143257.16	72236.97	28772.36	5417.36
Slope/ R^2			2.90×10^6/0.993		
QY			25.3%		

Table S2 The absorption intensity and PL intensity of quinine sulfate.

Quinine sulfate	1	2	3	4	5
Abs	0.069	0.041	0.035	0.023	0.017
Integrated PL	336485.79	147344.65	119974.82	42431.88	9330.6
Slope/ R^2			6.30×10^6//0.997		
QY			55%		

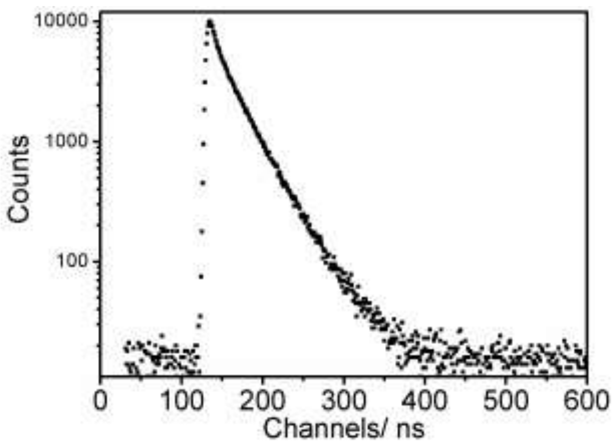

Fig. S8 Photoluminescence lifetime intensity decay of the g-CDs in aqueous solution (excitation at 370 nm, emission at 430 nm).

Table S3 The photoluminescence decay of g-CDs.

τ_i/ns	A_i/%
0.90	16.91
7.78	73.87
2.98	9.22

The average photoluminescence lifetime was obtained by the formula below:

$$\bar{\tau} = \frac{A_1\tau_1 + A_2\tau_2 + A_3\tau_3}{A_1 + A_2 + A_3}$$

Herein, the average Photoluminescence lifetime of the as-obtained g-CDs was 6.17 ns. where τ_i was the time-resolved decay lifetime, A_i was the proportion.

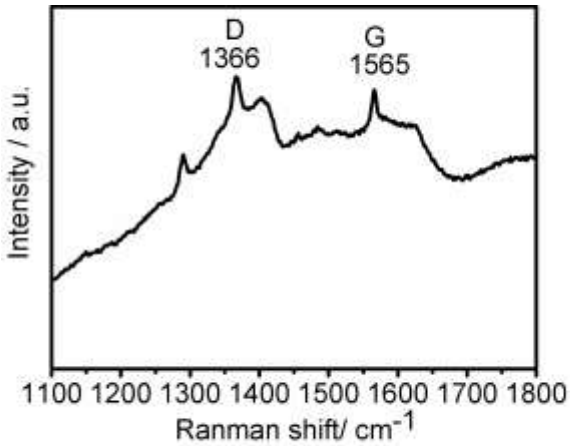

Fig. S9 Raman spectrum of the g-CDs, the Raman spectra are measured on the Ag substrate (use 532 nm laser as excitation wavelength).

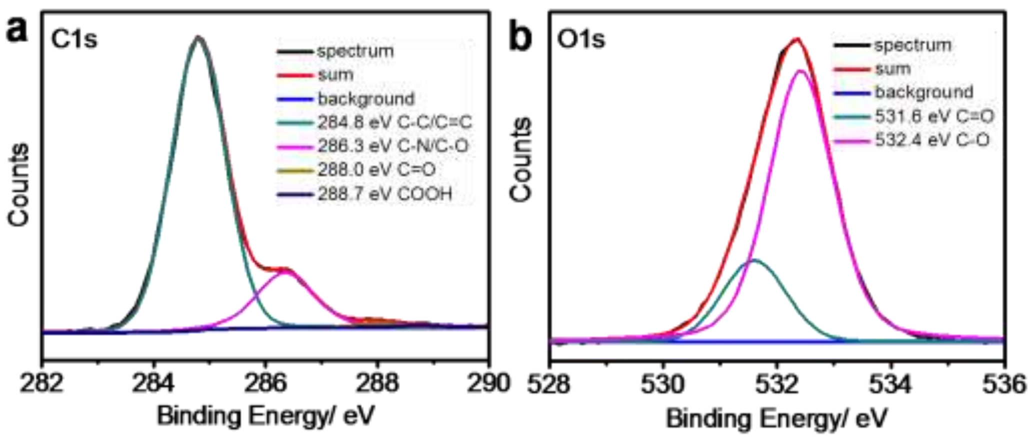

Fig. S10 High-resolution spectra of C1s (a) and O1s (b).

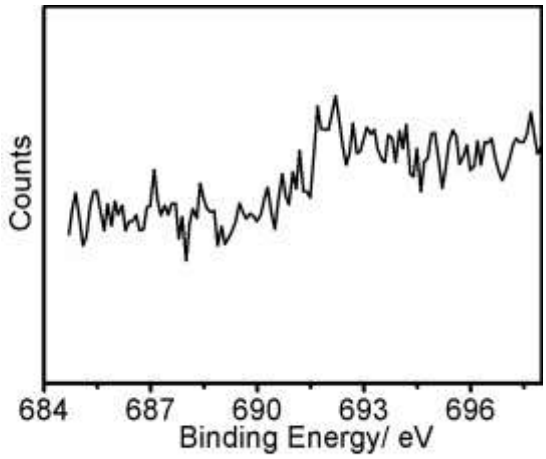

Fig. S11 Background signal of XPS without fluorine in the range of 685-698 eV.

Table S4 The relative amount of C, N, O, F of g-CDs determined by XPS

name	Atomic %
C1s	67.18
O1s	28.25
N1s	3.85
F1s	0.72

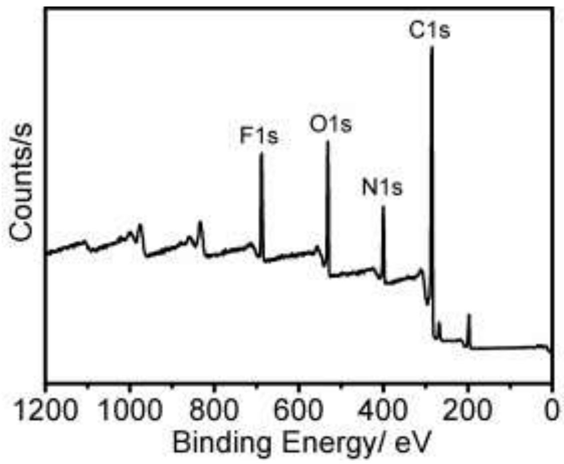

Fig. S12 XPS spectrum of ciprofloxacin hydrochloride determined by XPS.

Table S5 The relative amount of C, N, O, F of ciprofloxacin hydrochloride determined by XPS and their theoretical content (just take C, N, O, F into consideration).

name	XPS data (%)	Theoretical content (%)
C1s	68.74	65.18
O1s	11.59	15.34
N1s	10.93	13.41
F1s	8.75	6.07

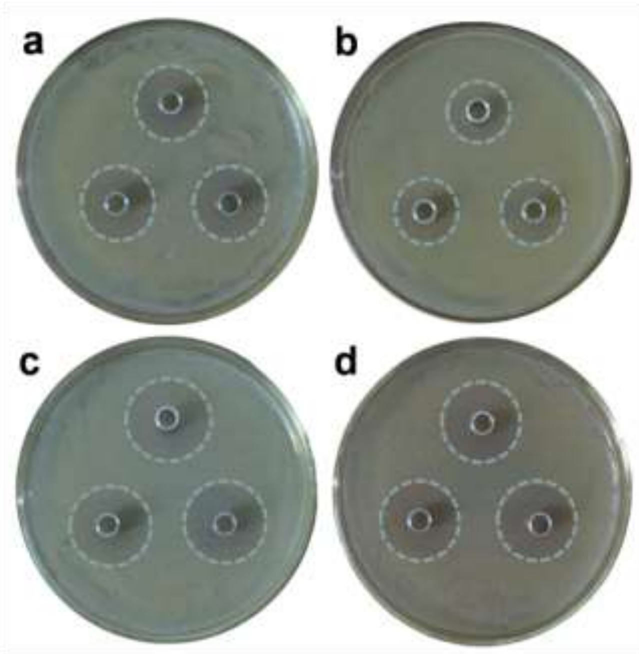

Fig. S13 Photographs of the diameter of inhibition zone for (a) g-CDs, *E. coli*; (b) g-CDs, *S. Aureus*; (c) ciprofloxacin hydrochloride, *E. coli*; (d) ciprofloxacin hydrochloride, *S. Aureus* (the concentration of ciprofloxacin hydrochloride and g-CDs are both 1.25 μg mL^{-1}).

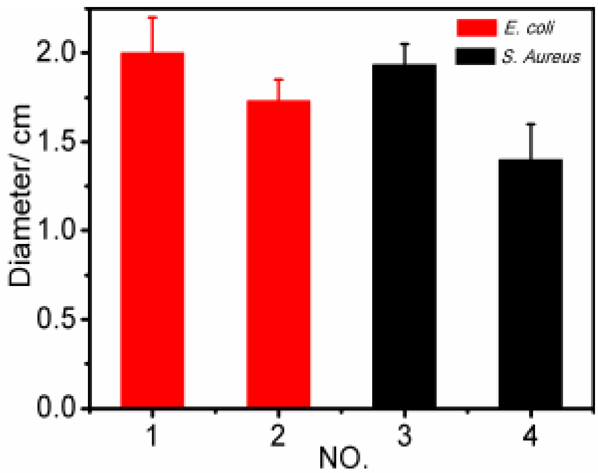

Fig. S14 Diameters of bacterial inhibition rings for ciprofloxacin hydrochloride and g-CDs. (No.1-4: 1 and 3, ciprofloxacin hydrochloride; 2 and 4, g-CDs)

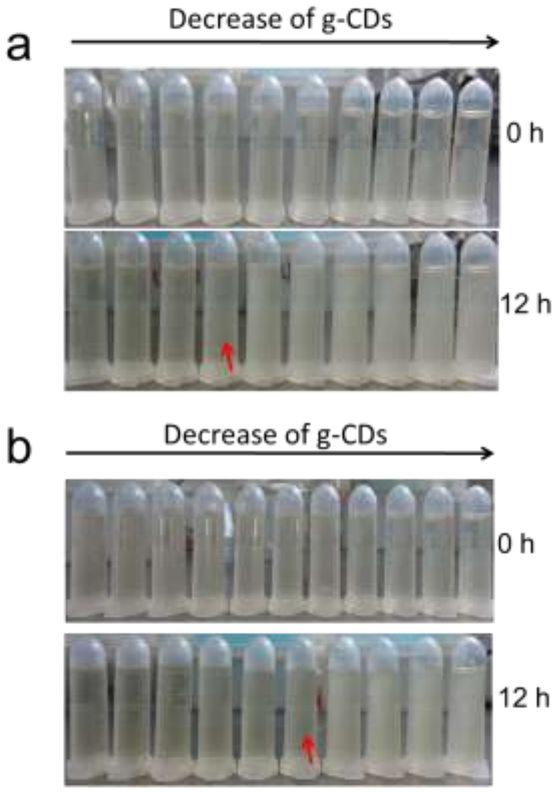

Fig. S15 Photographs of bacterial suspensions treated with different concentrations of g-CDs. (a) *S. aureus*, concentrations of g-CDs (from left to right, μg mL^{-1}): 8, 4, 2, 1, 0.5, 0.25, 0.125, 0.062, 0.031, 0. (b) *E. coli*, concentrations of g-CDs (from left to right, μg mL^{-1}): 0.8, 0.4, 0.2, 0.1, 0.05, 0.025, 0.0125, 0.0062, 0.0031, 0.

Table S6 Minimum inhibitory concentration (μg mL^{-1}) of g-CDs for two types of bacteria.

Strain	No.	MIC
S. aureus	ATCC 25,923	1.0
E. coli	ATCC 25,922	0.025

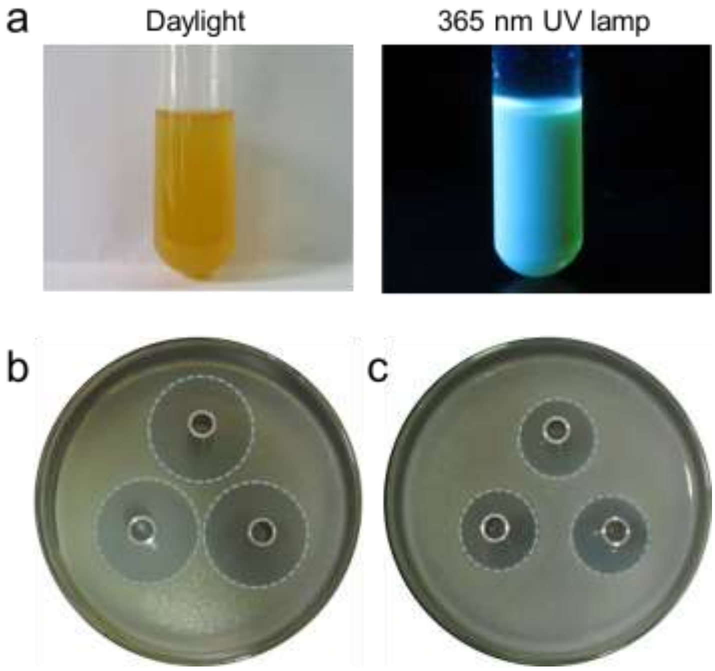

Fig. S16 The g-CDs purified by silica gel column chromatography (using dichloro-methane containing methanol as eluent). (a) Photographs of the purified g-CDs under daylight and 365 nm UV lamp. Photographs of the diameter of inhibition zone after cultured with purified g-CDs for *E. coli* (b) and *S. Aureus* (c), the concentration of g-CDs are 3 μg mL^{-1}.

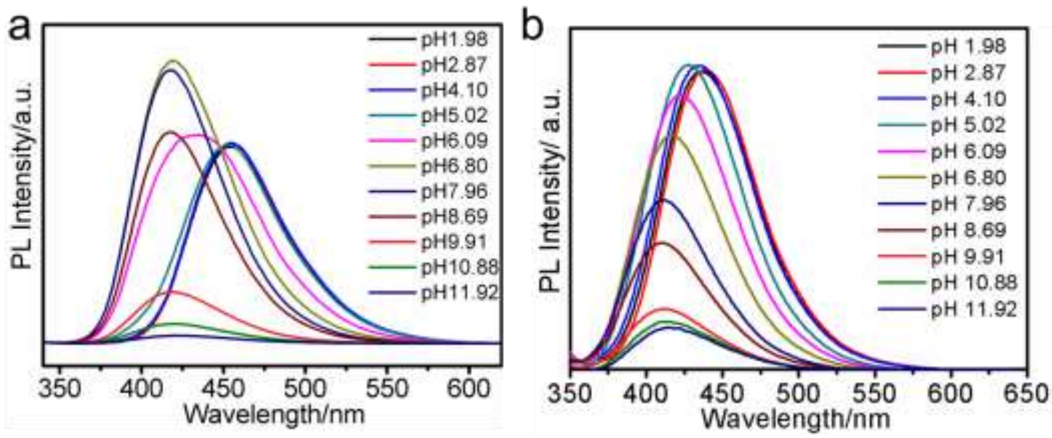

Fig. S17 The PL spectra of (a) ciprofloxacin hydrochloride and g-CDs (b) and under different pH BR buffer (1.98, 2.87, 4.10, 5.02, 6.09, 6.80, 7.96, 8.69, 9.91, 10.88, 11.92).

Table S7 Statistical characteristics from the Boltzmann fit.

Parameters	Value; S
a_0	7.988; 0.0501
a_1	723.270; 9.301
a_2	101.538; 4.534
a_3	0.818; 0.0562
R^2	0.998
Reduced X^2	11.437
Analytical range	1.98-11.92

S:standard error. a_0 and a_3 are adjusting coefficients.

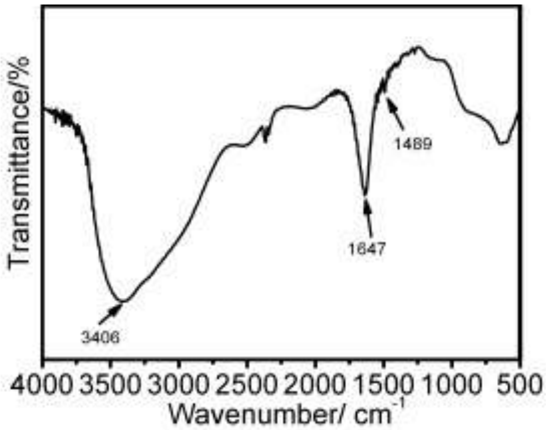

Fig. S18 FTIR spectrum of g-CDs after the coordination with Al^{3+} (dialysis through a dialysis membrane (500-1000 MWCO) over 2 days before determination of FTIR).

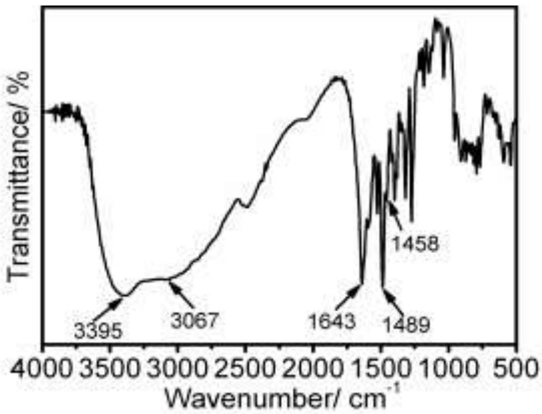

Fig. S19 FTIR spectrum of the ciprofloxacin after the coordination with Al^{3+}. The ciprofloxacin mixed with Al^{3+} has been dialyzed through a cellulose ester dialysis membrane (100 MWCO) over 2 days before the determination of FTIR.

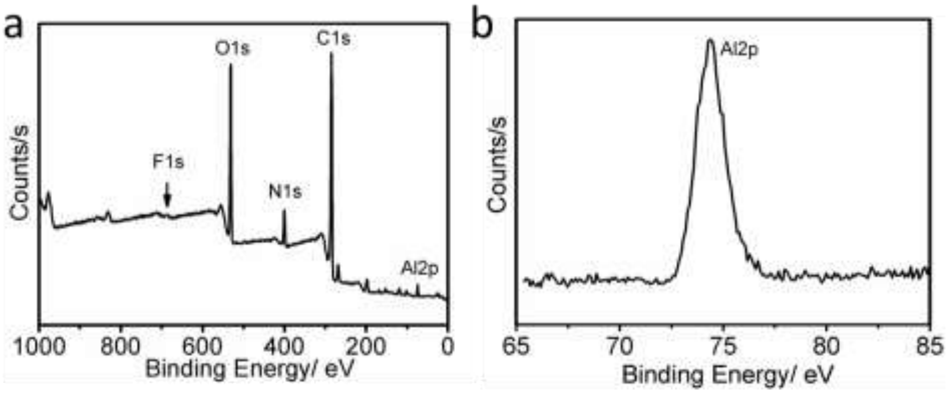

Fig. S20 (a) XPS spectrum of g-CDs after the coordination with Al^{3+} (dialysis through a dialysis membrane (500-1000 MWCO) over 2 days before determination of XPS). (b) High-resolution XPS spectrum of Al2p.

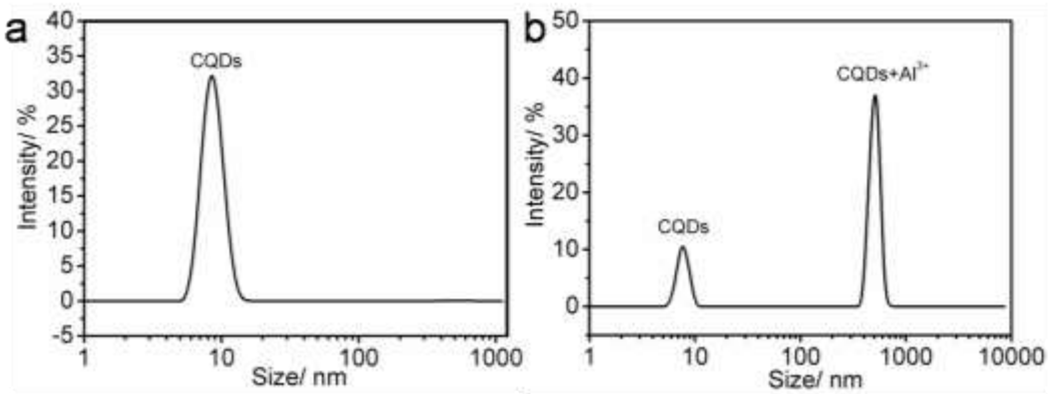

Fig. S21 Hydrodynamic diameters distribution of the g-CDs before (a) and after adding Al^{3+} (20 μM) (b).

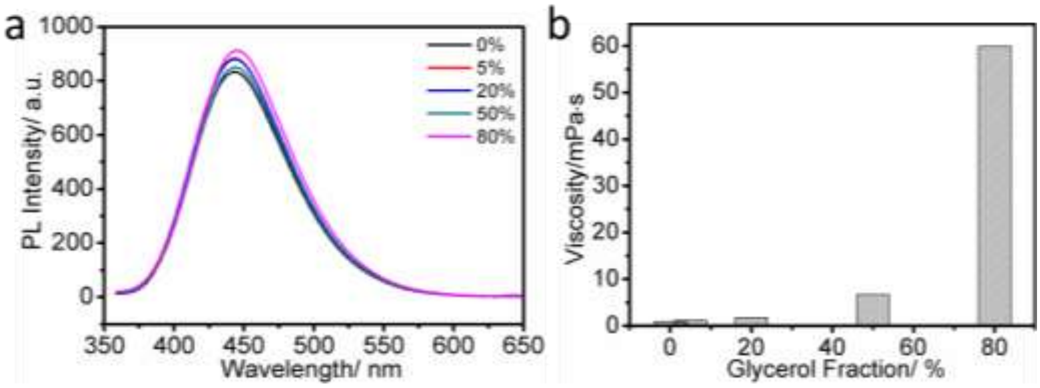

Fig. S22 (a) PL emission of g-CDs in glycerol/water mixtures of various proportions (glycerol %). (b) Viscosity of glycerol/water mixtures in different proportions.

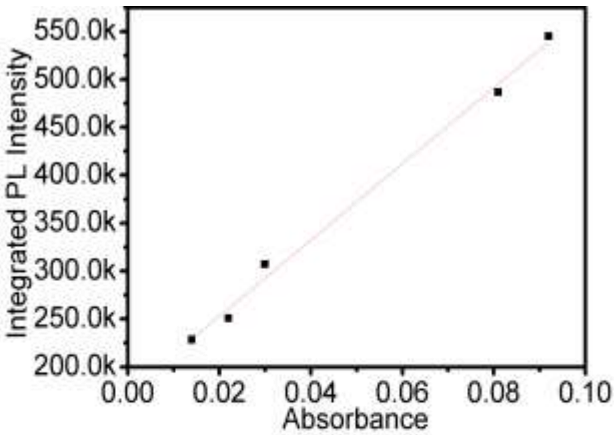

Fig. S23 Plots of integrated PL intensity versus absorbance of g-CDs after binding with Al^{3+} (λ_{ex}= 338 nm in water).

Table S8 The absorption intensity and PL intensity of g-CDs after binding with Al^{3+}.

g-CDs+Al^{3+}	1	2	3	4	5
Abs	0.092	0.081	0.033	0.022	0.014
Integrated PL	544874.11	486538.49	307026.97	250650.52	228378.71
Slope/ R^2			3.97×10^6/0.993		
QY			34.7%		

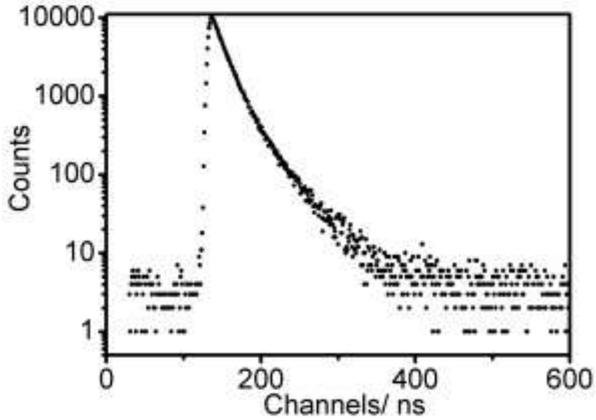

Fig. S24 Photoluminescence lifetime intensity decay of the g-CDs in the presence of Al^{3+} (excitation at 370 nm, emission at 430 nm).

Table S9 The photoluminescence decay of g-CDs in the presence of Al^{3+}.

τ_i/ns	A_i/%
3.94	54.35
6.94	35.24
10.4	10.42

Table S10 The rate constants of the g-CDs in aqueous solution in the presence of Al^{3+}.

	g-CDs	g-CDs+Al^{3+}
Φ/%	25.3	34.7
τ/ns	6.17	5.67
$k_r/10^6$ s^{-1}	41.0	61.2
$k_{nr}/10^8$ s^{-1}	1.21	1.15

Here τ stands for the average lifetime of CDs measured with excitation wavelength of 375 nm and emission wavelength of 430 nm, Φ stands for the QY of g-CDs using quinine sulfate as reference, k_r and k_{nr} refer to the radiative and non-radiative rate constants. The increase of radiative rate and the decrease of non-radiative rate obviously show the enhancement of PL efficiency according to following equation:[3]

$$K_r = \frac{\Phi}{\tau}$$

$$K_{nr} = \frac{1-\Phi}{\tau}$$

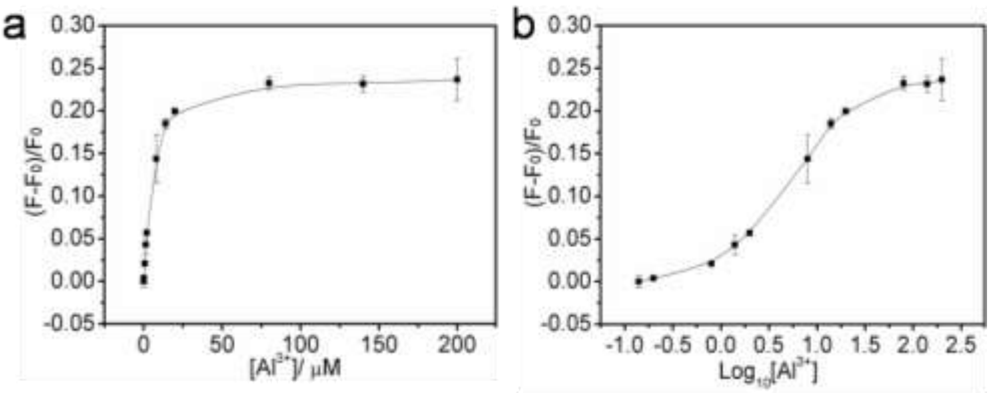

Fig. S25 (a) PL intensity ratio of g-CDs ($(F-F_0)/F_0$), where F_0 and F represent the PL intensity of the g-CDs in the absence and presence of Al^{3+}, respectively) in Different concentrations of Al^{3+}. (b) Plot of the PL intensity ratio of g-CDs *vs*. the logarithmic values of Al^{3+} concentrations.

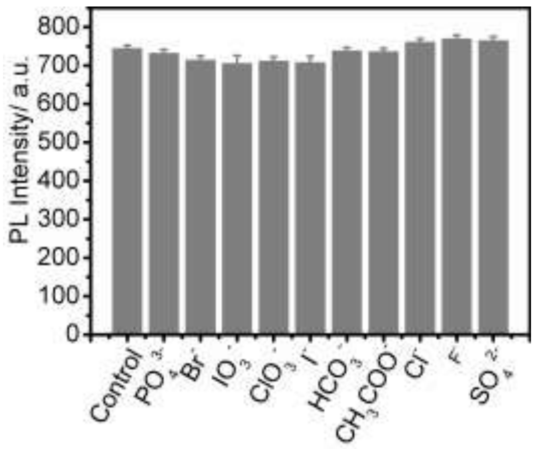

Fig. S26 The stability investigation of g-CDs toward different anions. PO_4^{3-}, Br^-, IO_3^-, ClO_3^-, I^-, HCO_3^-, CH_3COO^-, Cl^-, F^-, SO_4^{2-} ($[A]_a^{n-}$=100 μM, pH 5.02 BR buffer).

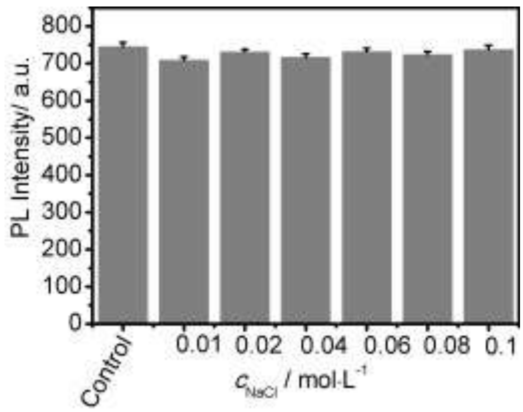

Fig. S27 The stability investigation of g-CDs toward sodium chloride solutions with different concentrations (0.01, 0.02, 0.04, 0.06, 0.08, 0.1 M).

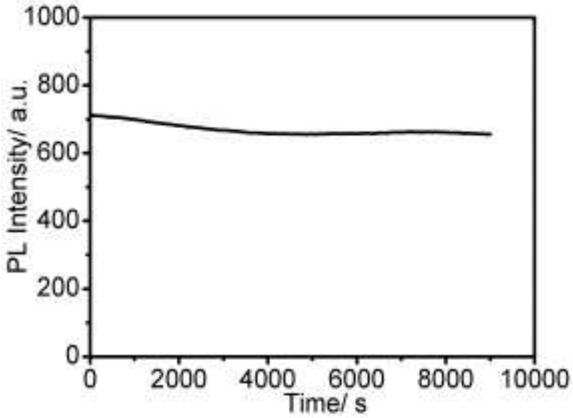

Fig. S28 Effect of time on the fluorescence intensity of g-CDs (excitation at 338 nm, emission at 432 nm, 150W Xe lamp).

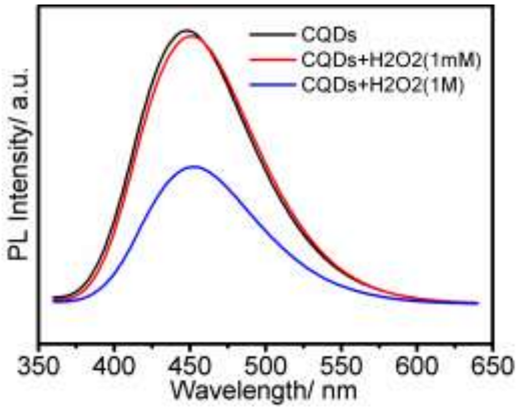

Fig. S29 Effect of hydrogen peroxide (1 mM, 1 M) on the PL intensity of g-CDs.

References

1. Z. L. Wu, P. Zhang, M. X. Gao, C. F. Liu, W. Wang, F. Leng and C. Z. Huang, J. Mat. Chem. B, 2013, 1, 2868-2873.
2. H. Ding, S.-B. Yu, J.-S. Wei and H.-M. Xiong, ACS Nano, 2016, 10, 484−491.
3. W. L. Cheng, S. J. Dong and E. K. Wang, Angew. Chem., Int. Ed., 2003,42, 449–452.